A Personalized Model for Galvanic Coupling in Intrabody Communication Systems

M. Amparo Callejón[1], David Naranjo[2,1], Javier Reina-Tosina[3,2], and Laura M. Roa[1,2]

[1] Biomedical Engineering Group, University of Seville, Seville, Spain
[2] CIBER de Bioingeniería, Biomateriales y Nanomedicina (CIBER-BBN), Spain
[3] Dept. of Signal Theory and Communications, University of Seville, Seville, Spain
{mcallejon,dnaranjo,jreina,lroa}@us.es

Abstract. Intrabody communication (IBC) uses the human body as a transmission medium for electrical signals, providing an efficient channel to interconnect devices in Body Sensor Networks. For IBC galvanic coupling, the signal path is accomplished through two pairs of electrodes deployed on the skin, which suggest the dependence of the attenuation signal on the subject's electrophysiological skin properties. With the purpose of gaining an insight into the attenuation differences observed for diverse subjects, a simple transmission line-based model has been used for the identification of those personalized parameters that best emulate the attenuation behavior. Experimental results for two different subjects have been carried out using a harmonized measurement set-up. Model simulations have shown to match measurement data more accurately when individualized instead standard skin parameters were used, thus highlighting the need to deal with personalized models in IBC research.

Keywords: electrophysiological properties, galvanic coupling, intrabody communication, measurement set-up, pathloss, personalized parameters, transmission line model.

1 Introduction

Pervasive monitoring along with Body Sensor Networks (BSN) have been established as the technological basis for the delivery of preventive and personalized health systems, which aim to improve patients' quality of life [1]. Nevertheless, some technical challenges regarding the design of small-size, power-saving and miniaturized intelligent wearable devices are yet to be solved [2]. In this sense, a promising technique called Intrabody Communications (IBC), which uses the human body as a transmission medium for electrical signals, allows low frequencies and low power signals to be used, thus reducing consumption, permitting miniaturization and avoiding interferences [3]. One key issue involving IBC research is the human body characterization as a communication channel. For this purpose, different models, which have shed light on signal propagation mechanisms through the human body, have been proposed in the literature [4–7].

B. Godara and K.S. Nikita (Eds.): MobiHealth 2012, LNICST 61, pp. 130–137, 2013.

However, an accurate validation has not always been possible due to the great dependence of the experimental results on both the measurement conditions and the test subject [4,6,8]. In this way, significant differences in pathloss data have been found due to each subject's particular anthropometrical characteristics (e.g., diameter and length of the arm, weight, sex,...) and the position of electrodes through the body [4,6]. For instance, previous results reported by the authors evidenced that the frequencies at which the minimum attenuation was obtained did not match for different subjects [9], thus highlighting the need for personalized models. In spite of the fact that all existing IBC models in the literature use the widely accepted parameters reported in [10], there is evidence that these models have not always been able to emulate the complex frequency behavior of attenuation, with discrepancies existing among diverse authors' outcomes and different subjects. In addition, in the case of galvanic coupling, the dependence of the attenuation results on the subject's physiological parameters has been found to be even higher [4,9], which could be explained by the fact that the signal path is confined to the skin when sensors are deployed on it.

In this work, a skin transmission line model previously reported by the authors [11] has been used in order to identify the personalized parameters that best match the frequency behavior of the pathloss found for different subjects. Consequently, the objective of this work has been to show that a better agreement can be accomplished by considering personalized instead of generalized parameters. In order to assess these parameters, galvanic coupling attenuation experiments for different subjects have been carried out using a harmonized set-up [12]. For the purpose of validation, a set of measurements over different distances between electrodes were obtained and a satisfactory agreement between the model's predicted behavior and the experimental data was found. Finally, the results of the personalized model and those obtained by using generalized parameters were compared in order to show the need to deal with personalized models in IBC research.

2 Material and Methods

2.1 Distributed Transmission Line Model

The model used in this work, which can be seen in Fig. 1, is based on a skin transmission line model [11]. It consists in the distributed insertion of skin cross-sectional admittances, $Y_{skin}(\omega)$, and skin longitudinal impedances, $Z_{skin}(\omega)$, along a longitudinal plane. Specifically, $Y_{skin}(\omega)$ is formed by a shunt circuit composed of a conductance $G(\omega)$ that represents the conductive pathways of the skin (sweat glands and the ionic channels that cross the cell membrane), and a susceptance $B(\omega)$ that accounts for the keratinized cells of the stratum corneum (SC) and the lipid bilayer [13]. In addition, $Z_{skin}(\omega)$ corresponds to a resistive characteristic $R(\omega)$ that emulates the signal propagation between adjacent admittances. Finally, Z_e, whose frequency response was taken from [14], models the electrode impedance, and Z_l represents the input impedance of the receiver.

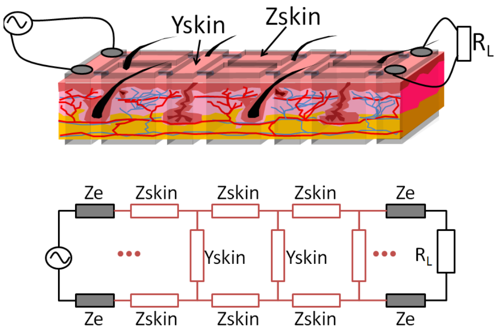

Fig. 1. Galvanic coupling transmission line model

A propagation constant $\gamma(\omega)$ can be found through

$$\gamma(\omega) = \sqrt{2Z_{skin}(\omega)Y_{skin}(\omega)} = \sqrt{2R(G(\omega) + jB(\omega))}\,, \tag{1}$$

where the constant factor of 2 is due to the differential characteristic of galvanic coupling.

In order to take into account the electrode effect through the Z_e impedances, which could cause an impedance mismatch, a reflection coefficient $\Gamma_l(\omega)$ was introduced in the model to obtain the total pathloss of the IBC system,

$$L(\text{dB}) = 20\log_{10}\frac{1 + \Gamma_l(\omega)e^{-2\gamma(\omega)l}}{(1 + \Gamma_l(\omega))e^{-\gamma(\omega)l}}\,, \tag{2}$$

where l is the length between electrodes.

The electrophysiological properties of the skin were addressed by means of $G(\omega) = K\sigma'(\omega)$, $R(\omega) = 1/G(\omega)$ and $B(\omega) = \omega\varepsilon_r'(\omega)\varepsilon_0 G(\omega)/\sigma'(\omega)$, where $K = A/d$, d is the transverse distance between the same pair of electrodes and A is the electrode measurement area. On the other hand, $\varepsilon_r'(\omega)$ and $\sigma'(\omega)$ are the real part of the permittivity $\hat{\varepsilon_r}(\omega)$ and the conductivity $\hat{\sigma}(\omega)$ of the skin, respectively. For the sake of simplicity, these were modeled by means of a single-pole Cole-Cole model given by (3) and (4), instead of the usual two-pole model reported in [10]. This simplification was validated within a limited frequency range, taking into account that galvanic coupling usually operates at frequencies up to 1 MHz, where a single-dispersion model is accurate enough.

$$\hat{\varepsilon_r}(\omega) = \varepsilon_\infty + \frac{\triangle\varepsilon_1}{1 + (j\omega\tau_1)^{1-\alpha_1}} + \frac{\sigma_s}{j\omega\varepsilon_0}\,, \tag{3}$$

$$\hat{\sigma}(\omega) = j\omega\varepsilon_0\hat{\varepsilon_r}(\omega)\,, \tag{4}$$

where ε_0 is the permittivity of vacuum. Subsequently, the rest of parameters in (3)-(4), were personalized for different subjects, instead of using the usual parameters reported in [10].

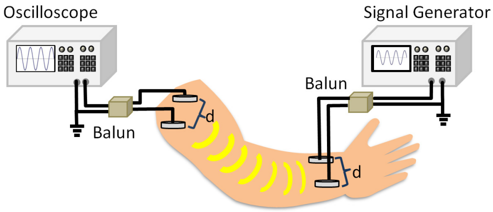

Fig. 2. Galvanic coupling measurement set-up

2.2 Galvanic Coupling Measurement Set-Up

The galvanic coupling measurement set-up, shown in Fig. 2, consisted of a GFG-8015G function generator of GW Instek to provide the signal, an MSO6032A digital oscilloscope of Agilent Technologies Inc. ($R_{input} = 1$ MΩ) to acquire it, a pair of PT4 balun transformers of Oxford Electrical Products and four electrodes. The baluns were used to remove the effect of the internal ground of both the signal generator and the oscilloscope, in order to obtain a realistic IBC galvanic coupling transmission path. Commercial round pregelled silver/silverchloride Swaromed ECG electrodes (0.5 cm-radius) were chosen. The two transmitter electrodes were attached to the skin near the wrist and the two receiving electrodes were moved along the forearm using two distances: 5 and 10 cm. At the same time, a distance of 9 cm between the two electrodes of the same pair was chosen, according to [12]. A sinusoidal signal with a peak-to-peak current amplitude of 0.5 mA was applied. Twelve frequency points from 20 kHz up to 1 MHz were considered. This limited frequency range was chosen because of the evidence that the human body acts as an antenna for higher frequencies [15, 16] and, in addition, some other non-deterministic effects, such as radiation from cables and electrodes, become non-negligible as frequency increases [17]. Finally, some anthropometrical characteristics such as sex, age, height, weight, arm length and arm diameter were taken into account, and are summarized in Table 1, for two subjects A and B. Finally, it must be noted that the amplitude levels considered in this work were established well in the bounds of the International Commission on Non-Ionizing Radiation Protection's (ICNIRP) regulations [18].

Table 1. Test subjects' anthropometrical characteristics

Subject	Sex	Age	Height	Weight	Arm length	Arm diameter
A	Male	33	1.82 m	100 kg	65 cm	9.5 cm
B	Female	27	1.57 m	50 kg	50 cm	4.3 cm

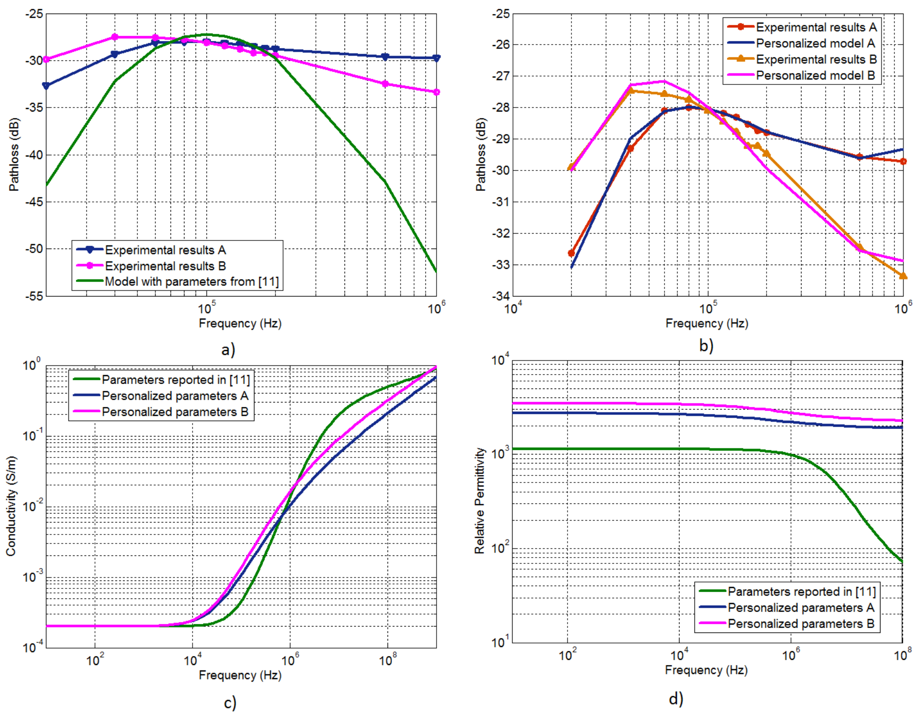

Fig. 3. (a) Comparison between experimental results and model simulations for subjects A and B. (Marks: measurement data; solid line: model with generalized parameters and $K = A/d$; dashed line: model with generalized parameters and $K = 0.7A/d$) (b) Comparison between experimental results and model simulations by using personalized parameters for subjects A and B. (c) Comparison between conductivity model by using generalized and personalized parameters for subjects A and B. (d) Comparison between permittivity model by using generalized and personalized parameters for subjects A and B.

Table 2. Personalized Parameters for (3)

Parameter set	ε_∞	$\triangle\varepsilon_1$	τ_1 (ns)	α_1	σ_s
Dry skin	37	1122	32.51	0.18	0.0002
Subject A	1855.81	876.32	325.11	0.49	0.0002
Subject B	2225.81	1246.32	230.61	0.45	0.0002

3 Results

We first implemented a Least-Mean-Square (LMS) algorithm to find the parameters from which the simplified single-pole Cole-Cole model was able to accurately

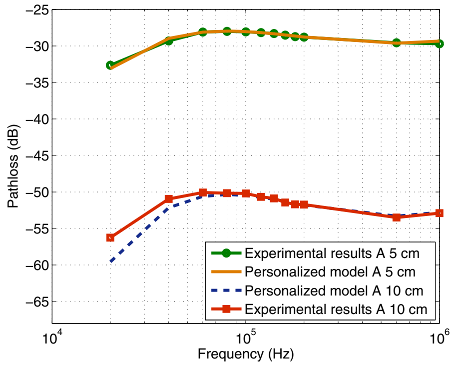

Fig. 4. Experimental results and model simulations obtained for subject A and two different distances of 5 and 10 cm between electrodes

reproduce both skin permittivity and conductivity reported in [10]. These parameters, whose values are given in Table 2 (Dry Skin), showed to be valid up to 1 GHz, which is much higher than the usual galvanic coupling frequency band (up to 1 MHz) [4,6,9]. Once the validity of this simplification was proven, we subsequently used the same LMS algorithm to identify the personalized parameters that best match the model's pathloss curve to that obtained experimentally, for both subjects A and B. These parameters are also listed in Table 2 (Subjects A and B). The pathloss curves obtained by using the generalized parameters in [10] are shown in Fig. 3a, whereas those obtained by using personalized parameters are shown in Fig. 3b. It can be seen that in the former case, personalization was addressed through the parameter K, considering a smaller measurement area (parameter A) for subject B, whose arm diameter was lower. The characteristics obtained for $\hat{\varepsilon_r}(\omega)$ and $\hat{\sigma}(\omega)$ using the single-pole Cole-Cole model along with the personalized parameters found for each subject are shown in Fig. 3c and 3d. Furthermore, in order to validate the model with personalized parameters, other experimental samples by changing the distance between the electrodes were considered. Therefore, once the personalized parameters were found for the given subjects, they were subsequently applied to the model in order to predict the experimental results obtained with a separation of 10 cm between the electrodes. The results for subject A and two different distances are shown in Fig. 4.

4 Discussion

The attenuation results obtained from using generalized parameters in Fig. 3a show that only a satisfactory agreement is obtained within 50-250 KHz, as was previously evidenced in [9]. This could be due to the fact that the signal path is primarily accomplished through the skin within this frequency range, and out of which other signal paths begin to be dominant. In fact, the signal could even penetrate through the skin towards the muscle or the fat, notwithstanding that there also exist other external phenomena such as off-body radiation that could affect at higher frequencies. On the other hand, it must be noticed how the maximum peak of the pathloss curve is located at different frequencies for different subjects, as can be seen in Fig. 3b. It can also be noticed how the use of personalized parameters yields to a better fit between model and experimental results in the galvanic coupling approach. This may be explained by the fact that they are capable of reproducing the dominant effect of different tissues within a wider frequency range. In much the same way, these parameters address some underlying issues related not only to the subjects' anthropometrical characteristics, but also to the electrophysiological properties of the skin. In fact, skin admittance varies considerably between different people and different environmental conditions. Changes in hydration mechanisms due to sweat gland activity and temperature can be manifested in large variations of skin admittance [19]. Nevertheless, the trends observed for the dielectric properties of skin by using personalized parameters were found to be quite similar to those reported for skin in [10], thereby producing a response within a physiological range, as can be seen in Fig. 3c and 3d. Finally, the results for subject A shown in Fig. 4 highlight that there exists a satisfactory agreement for both distances, thus showing the validity of the model using personalized parameters.

5 Summary and Conclusion

In order to gain an insight into the differences observed for diverse subjects, a simple IBC galvanic coupling model has been used in this paper. With this objective in mind, an LMS algorithm was implemented in order to find those personalized parameters that best adapt the model's response to the experimental results. In fact, we have shown that it is necessary to personalize the models not only regarding anthropometrical characteristics but also skin dielectric properties. In addition, the conductivity and permittivity obtained by means of these parameters showed to have a similar trend to that reported in [10]. Finally, experimental results considering another distance between electrodes were used in order to validate such personalized parameters. The satisfactory agreement between the model's response and the experimental results shows the validity of the proposed approach and suggests the use of personalized models in order to overcome some of the discrepancies observed between authors' outcomes in IBC literature.

Acknowledgments. The authors are grateful to E.C. Wiegers, G. Barbarov and D. Plant for their useful comments and help. This work was supported in part by the Consejería de Economía, Innovación y Ciencia, Government of Andalucía, under Grants P08-TIC-04069 and P10-TIC-6214.

References

1. Maglaveras, N., Bonato, P., Tamura, T.: Guest Editorial Special Section on Personal Health Systems. IEEE Trans. Inf. Technol. Biomed. 14, 360–363 (2010)

2. Li, S., Hu, F., Li, G.: Advances and Challenges in Body Area Network. In: Zhang, J. (ed.) ICAIC 2011, Part III. CCIS, vol. 226, pp. 58–65. Springer, Heidelberg (2011)
3. Zimmerman, T.G.: Personal area networks: Near-field intrabody communication. IBM Systems Journal 35(3.4), 609–617 (1996)
4. Song, Y., Qun Hao, Q., Zhang, K., Wang, M., Chu, Y., Kang, B.: The Simulation Method of the Galvanic Coupling Intrabody Communication With Different Signal Transmission Paths. IEEE Trans. Instrum. Meas. 60, 1257–1266 (2011)
5. Xu, R., Hongjie Zhu, H., Yuan, J.: Electric-Field Intrabody Communication Channel Modeling With Finite-Element Method. IEEE Trans. Biomed. Eng. 58, 705–712 (2011)
6. Pun, S.H., Gao, Y.M., Mak, P.U., Vai, M.I., Du, M.: Quasi-Static Modeling of Human Limb for Intra-Body Communications With Experiments. IEEE Trans. Inf. Technol. Biomed. 15(6), 870–876 (2011)
7. Bae, J., Cho, H., Song, K., Lee, H., Yoo, H.-J.: The Signal Transmission Mechanism on the Surface of Human Body for Body Channel Communication. IEEE Trans. Microw. Theory Tech. 60(3), 582–593 (2012)
8. Lucev, Z., Krois, I., Cifrek, M.: Effect of body positions and movements in a capacitive intrabody communication channel from 100 kHz to 100 MHz. In: IEEE International Instrumentation and Measurement Technology Conference (I2MTC), pp. 2791–2795 (2012)
9. Callejón, M.A., Naranjo, D., Reina, J., Roa, L.M.: Distributed Circuit Modeling of Galvanic and Capacitive Coupling for Intrabody Communication. IEEE Trans. Biomed. Eng. PP(99), 1 (2012); early access article
10. Gabriel, S., Lau, R.W., Gabriel, C.: The dielectric properties of biological tissues: III. Parametric models for the dielectric spectrum of tissues. Physics in Medicine and Biology 41, 2271 (1996)
11. Callejón, M.A., Roa, L.M., Reina, J., Naranjo, D.: Study of Attenuation and Dispersion through the Skin in Intra-Body Communications Systems. IEEE Trans. Inf. Technol. Biomed. 16(1), 159–165 (2012)
12. Callejón, M.A., Naranjo, D., Reina-Tosina, L.J., Roa, L.M.: A First Approach to the Harmonization of Intrabody Communications Measurements. In: Long, M. (ed.) World Congress on Medical Physics and Biomedical Engineering May 26-31, 2012 Beijing, IFMBE Proceedings, vol. 39, pp. 704–707. Springer, Heidelberg (2013)
13. Grimnes, S., Martinsen, Ø.G.: Bioimpedance and bioelectricity basics, pp. 105–109. Ed. Academic Press (2000)
14. Hachisuka, K., Takeda, T., Terauchi, Y., Sasaki, K., Hosaka, H., Itao, K.: Intrabody data transmission for the personal area network. Microsystem Technologies 11, 1020–1027 (2005)
15. Cho, N., Yoo, J., Song, S.-J., Lee, J., Jeon, S., Yoo, H.-J.: The Human Body Characteristics as a Signal Transmission Medium for Intrabody Communication. IEEE Trans. Microw. Theory Tech. 55, 1080–1086 (2007)
16. Koutitas, G.: Multiple Human Effects in Body Area Networks. IEEE Antennas Wireless Propag. Lett. 9(5), 1080–1086 (2007)
17. Xu, R., Ng, W., Zhu, H., Shan, H., Yuan, J.: Environment Coupling and Interference on the Electric-Field Intrabody Communication Channel. IEEE Trans. Biomed. Eng. 59(7), 2051–2059 (2012)
18. International Commission on Non-Ionizing Radiation Protection: Guidelines for Limiting Exposure to Time-Varying Electric, Magnetic, and Electromagnetic Fields (up to 300 GHz). Health Physics 74(4), 494–522 (1998)
19. Tronstad, C., Johnsen, G.K., Grimnes, S., Martinsen, Ø.G.: A study on electrode gels for skin conductance measurements. Physiol. Meas. 31, 1395 (2010)